

# An integrated prognostics method for failure time prediction of gears subject to the surface wear failure mode

Fuqiong Zhao, Zhigang Tian<sup>\*</sup>, Xihui Liang, Mingjiang Xie

Department of Mechanical Engineering, University of Alberta  
Edmonton, Alberta, T6G 1H9, Canada

## **Abstract**

Surface wear is one of the main failure modes that gears suffer from due to sliding contact in the mesh process. However, the existing gear prognostics methods mainly focused on the fatigue cracking failure mode, and the existing prediction methods considering surface wear are physics-based without utilizing condition monitoring data. This paper proposes the first integrated prognostics method for failure time prediction of gears subject to surface wear failure mode, utilizing both physical models, i.e. the Archard's wear model, and condition monitoring data, i.e. inspection data on gear mass loss in this study. By noticing the importance of wear coefficient in Archard's model, the proposed method can result in a more accurate value of the wear coefficient so that the wear evolution in the future is forecasted with more accuracy. To achieve this, a Bayesian update process is implemented to incorporate the mass loss observation at an inspection point to determine the posterior distribution of the wear coefficient. With more mass loss data available, this posterior distribution gets narrower and its mean approaches the actual value of the coefficient. To use Archard' model, the gear mesh geometry and Hertz contact theory are applied to compute sliding distance and contact pressure for different points on the

---

<sup>\*</sup> The corresponding author (email: ztian@ualberta.ca).

tooth flank. The proposed method is validated using run-to-failure experiments with a planetary gearbox test rig.

**Keywords:** integrated prognostics, gear, surface wear, condition monitoring, physics-based, experimental validation

## 1. Introduction

Gears, as fundamental building blocks in mechanical power transmission systems, are widely used in various industrial applications. The health of gears is important for the safety of engineering systems. With the mission of transmitting heavy load, gears mainly suffer from four types of failure modes: surface wear, bending fatigue (fatigue cracking), contact fatigue and scoring [1]. Existing studies on gear failure time prediction, including modeling and experiment validations, were mainly focused on the fatigue cracking failure mode. In this paper, we mainly consider the surface wear failure mode, which also plays an important role in gear failures.

During the mesh process of gear pairs, the tooth flanks are loaded to contact with each other. The gear surface movement is a combination of rolling and sliding motions. When the surface velocities of the two contact teeth are different, the sliding component is introduced. The sliding contact will cause the material removal from the gear teeth and hence the gear mass is reduced. For the case of involute profile in spur gears, all the points on the tooth flank experience sliding movement except for the pitch point. At the pitch point, pure rolling condition occurs because the sliding velocity is zero. Material loss will alter the gear tooth profile geometry, and hence the dynamic characteristics of the gearbox. As a consequence, the level of vibration and noise will increase, and furthermore, other failure mechanisms may also be accelerated.

The prediction of gear wear propagation is of great interest for effective maintenance after the transmission systems is deployed in service. With the information about the wear depth on gear teeth predicted in advance, we can evaluate the dynamic performance of gearbox in the future and timely arrange the repair or the replacement schedule to avoid unexpected further damage and downtime. Given a threshold of the wear severity, the remaining useful life (RUL) of the gear will be estimated accordingly. The prediction of component RUL associated with the prediction confidence estimation is the objective of component prognostics and health management.

The existing prognostics methods can be grouped into three categories: physics-based methods, data-driven methods and integrated methods. The three categories are adopted typically in different scenarios when considering the availability of physical models, failure histories, condition monitoring data and computational complexity.

Physics-based methods use damage propagation models based on the physic laws of failure mechanism. The well-known Paris' law [2] is the one that is widely used to describe the fatigue crack growth with time. By defining a threshold value of crack size, the failure time of the component bearing this crack can be predicted. In [3], the authors studied factors that could have influences on crack propagation path in the gear tooth, including backup ratio, initial crack location, fillet geometry, rim/web compliance, gear size and pressure angle. The research in [4] considered the effect of moving load on the crack growth prediction. The authors divided the tooth engagement phase into multiple steps to obtain accurate values of stress intensity factor (SIF), which is the most important quantity in Paris' law. Finite element (FE) methods were implemented to handle stress intensity factor calculation under complex loading. Interested readers can refer to [5-7] for more details on the special element type in FE method for SIF

computation near the crack tip. In addition to improving the accuracy of SIF, researchers also investigated ways of estimating crack sizes through condition monitoring to better estimate RUL. In work [8], authors developed methods to estimate the current crack size by analyzing gearbox transmission error. Kacprzyński et al. [9] proposed a prognostic method that can predict gear failure probability by fusing physics-of-failure models and diagnostics information. However, due to complicated damage initiation and propagation processes, physics-based methods are restricted to very limited areas of simple and specific applications. It also costs extra efforts in large amount of experiments to determine the parameters used in the physical laws.

Data-driven methods apply when sufficient failure histories or condition monitoring data are available, based on which we can compute the failure distribution or form the relationship between ages and CM data. Banjević et al. [10] proposed a proportional-hazards model with time dependent stochastic covariates as lifetime model to predict the component failure rate and to optimize the replacement policy. Gebraeel et al. [11] selected the degradation model as exponential in which the parameters were updated using a Bayesian approach. In addition to the degradation models with pre-defined mathematical form, the data-driven models that are established through machine learning are also playing an important role for large data sets. Gebraeel and Lawley [12] developed neural networks to predict bearing failure time, which aimed to train a relationship between the bearing service time and the corresponding vibration spectrum. Tian et al. [13] developed a neural network to predict RUL using both failure and suspension condition monitoring histories. Wang et al. [14] investigated neuro-fuzzy approach and recurrent neural network for gear prognostics with various failure modes. An extended recurrent neural network was proposed to predict the health condition of gears in [15], in which the Elman context layer was incorporated to enhance its ability to model nonlinear time series.

Xi et al. developed a copula-based sampling method for data-driven prognostics, where a Copula-based statistical model was proposed for degradation modeling and simulation-based method was employed for remaining life prediction [16]. These processes require data to be sufficient so as to gain the statistical property, and otherwise the prediction could be unsatisfactory. The scarcity of failure histories, time-varying operating conditions and thresholding setting are examples of challenges for data-driven methods to be effective.

By noticing the merits and shortcomings of these two above-mentioned methods, integrated methods are proposed to combine physics of failure and condition monitoring data to benefit from both. In integrated methods, the physical model parameters are treated as random variables, and they are updated using condition monitoring data so as to approach their real values. Bayesian framework fits well to achieve the goal of integrated prognostics because of its natural environment for sequential learning and uncertainty quantification. Therefore, it is widely used in integrated prognostics. Coppe et al. [17] studied the problem of crack propagation in aircraft fuselage panel, where Bayesian inference was used to estimate parameters in Paris' law and error term with assumption of independence of model parameters. Later on An et al. [18] extended the methods to consider the correlation between model parameters. In authors' prior work [19], integrated prognostics methods were proposed for gear health prediction and uncertainty quantification. The authors then proposed to use polynomial chaos expansion to improve the efficiency of Bayesian update process in prognostics [20]. To handle the time-varying operating conditions, an approach was devised in [21] to make the integrated prognostics applicable in various loading environment. Bayesian inference also applied to study the spall propagation in bearings [22]. In recent years there is an increasing volume of publications that used dynamic systems as degradation models because of its natural interface with real-time condition

monitoring data. In [23], the Kalman filter was implemented to update RUL prediction of bearings using vibration signature as observations. Prognostic models in [24-26] are established in a particle filtering framework, in which the problem of non-linear state transition and non-Gaussian noise can be tackled.

In this paper, an integrated prognostics method is developed to predict the wear propagation on gears. Researchers have proposed various wear models which are dedicated to forecasting the wear progression with time [27]–[38], most of which can be classified as physics-based methods. Archard’s wear model proposed in [27] is a simple but classic model based on the theory of asperity contact. It expressed the worn volume as a function of sliding distance, applied load and hardness of materials. The coefficient in Archard’s model was related to the probability that the two asperity would produce a wear particle. A summary of understanding in wear modeling for metals was presented in [28]. The paper also proposed future research areas for metal wear prediction. Authors in [29] examined two mechanical wear processes, severe abrasive wear and mild sliding wear, to show that due to variety and complexity of the mating surface conditions, tests are actually needed to determine the parameters in wear propagation laws. In [30], the authors did an analysis on steel surface using scanning electron microscopy and auger electron microscopy and proposed mathematical expressions for the wear rate. The author in [31] discussed the wear resistance, wear model and wear rate using experimental results, and explained the wear phenomenon from the viewpoints of plastic deformation and fracture. The sliding model proposed in [32] considered two wear mechanisms: thermal desorption at low contact temperature and oxidative mechanism at elevated contact temperature. The micro-EHL effects were included by simulating two rough surfaces using digitized surface roughness profiles. Authors of [33] investigated sliding wear from micromechanics level. Periodic unit cell-

type continuum mechanics models were used to obtain the wear rate. A wear model was proposed in which the authors researched the influence on the wear rate of the principal material, loading and surface roughness. In [34], analytical time domain models were used to predict wear status in transient and steady-state operating conditions. A sliding polymer-based contact was adopted in the wear model. The author in [35] developed a mathematical model to correlate the material volumetric loss due to wear with the dissipation energy in sliding contacts. Two mechanisms of energy loss were considered: plastic deformation and elastic energy of the particulate. This model can be used to predict the service life of components and structures. The finite element model developed in [36] generalized Archard's law by allowing hardness of the soft material to be a function of temperature. The model in [37] used a free mesh to investigate the sliding wear in a composite alloy. The authors in [38] considered mechanical wear between two materials at high velocity. Apart from the above-mentioned physics-based models, data-driven methods are also presented to investigate the relationship of wear loss and potential effective conditions. For example, empirical models of wear rate were obtained by response surface method [39], [40] and artificial neural networks were used in [41], [42].

Among the preceding research work, Archard' wear model [27], [31] is now generally accepted as a suitable framework within which quantitative analysis on wear progression can be discussed [43]. The Archard' model was further generalized to regard the wear process as an initial value problem in [44] and was described by a differential equation as

$$\frac{dh}{ds} = kp. \quad (1)$$

where  $h$  is the wear depth,  $s$  is the sliding distance,  $k$  is a dimensional wear coefficient, and  $p$  is the contact pressure. It is clear that to obtain the wear depth of a point on tooth flank, (1) requires

the values of contact pressure  $p$  and sliding distance  $s$ . The wear coefficient  $k$  is an important parameter that determines the wear rate. As mentioned before, parameter determination is a serious task in physics-based prognostics. Because there exists a large amount of variation in the value of wear coefficient among different units due to contacting material property, experiments are needed for wear coefficient determination. As far as physics-based methods are concerned, once the coefficient is obtained through experiment, it will be fixed as a material dependent constant ready to use for other components. This assumption apparently neglects the variation or uncertainty in material properties, surface conditions and lubrication conditions. Hence, using a fixed wear coefficient did not consider the uncertainty in the wear propagation process, and change in the coefficient will have big impact on wear propagation and thus failure time prediction. This paper will overcome this problem by treating wear coefficient as a random variable, whose distribution is adjustable according to the condition monitoring data specific to the component of interest. Although the wear coefficient distribution for the population may be wide, it will be very narrow or even deterministic for a specific gear unit under consideration, and we intend to determine that using the proposed integrated prognostics method. Next we will give a brief review on physics-based methods using Archard's model as well as a summary of the proposed integrated method.

The Archard' model was used to predict the wear in spur and helical gears in [45], [46] respectively. For the spur gear model, the sliding distance is calculated based on involute profile. The contact pressure was obtained by a Winkler surface model. When calculating the load on gear tooth, the mesh stiffness was assumed to be constant for simplicity. The wear coefficient  $k$  is selected as a parameter with constant value. There were no experiment results reported in these two papers to validate the method. A wear prediction methodology was proposed in [1] for

parallel axis gear pairs, which was also based on Archard' model. In the paper, commercial software was employed to calculate contact pressure during gear mesh process. Thanks to the finite element model and technique of surface integral formulation, the method was able to calculate the contact pressure and the sliding distance while accounting for the geometry change due to wear and tooth manufacturing imperfections. In the experimental validation, four tests were conducted. The purpose of the first experiment was to determine the wear coefficient  $k$ . The predictions were conducted using the same  $k$  obtained in the first experiment and were compared to the other three tests because the authors assumed that all the test specimens were manufactured with the same material, heat treatment, and manufacturing process, and also assumed the same test conditions. These assumptions exclude the variations of wear coefficient among different units and impose risks of applying this wear coefficient to other units.

In this paper, we consider the wear coefficient as a random variable to account for its variation in different units. However, for a specific unit, the uncertainty of the wear coefficient value is much less than that of the population. Therefore, we propose to use inspection data during the wear process to reduce the uncertainty in wear coefficient for the specific unit. Because the wear removes material of contacting surface, the mass loss would be an effective indicator for the wear status. Mass loss can be obtained by measuring the weight of the gear offline, or by online monitoring system to measure the quantity of metal particles. The mass loss data will be integrated into a Bayesian inference to update the prior distribution of the wear coefficient into its posterior distribution. The posterior distribution is expected to better characterize the specific wear process as a result of the data integration.

The remainder of the paper is organized as follows. In Section 2, the integrated prognostics framework is presented, which shows the logic of the integration of physical models and

condition monitoring data. Section 3 illustrates how the wear coefficient is updated in the model update process through Bayesian inference. In Section 4, the physical models for wear prediction of a spur gear are established. Section 5 presents the method validation using run-to-failure experiments on a planetary gearbox test rig. Section 6 concludes the work.

## **2. Integrated prognostics method for gear wear prediction**

Compared to data-driven prognostics methods, predictive models that are based on physics of failure bear better accuracy, but requires efforts to build physical models, which could be very complex, and determine the model parameters. The idea of integrated prognostics is to integrate physical models and data from multiple sources to predict the damage progression and remaining useful life. As mentioned before, the most commonly used way to integrate physical models and data is the Bayesian inference approach [17-26], [47]. The framework of the proposed integrated prognostics method in this paper is shown in Figure 1. There are three parts in this framework: physical models, data and update process. In the part of physical models, the wear progression model, that is the Archard's wear model, is used to predict the wear depth evolution. The wear coefficient  $k$  is treated as a random variable. The sliding distance and contact pressure used in Archard's model are calculated based on gears mesh geometry and contact process. In the part of data, two types of data are listed. The data of failure history could give us prior information of wear coefficient value as a statistical property of gear population. In contrast, the inspection data is collected from the specific individual gear that is currently in use. In this paper, the mass loss of spur gear at inspection times serves as the inspection data. The purpose of the model update part is to use Bayesian inference to update the distribution of wear coefficient by taking in the inspection data as observations in the inference.

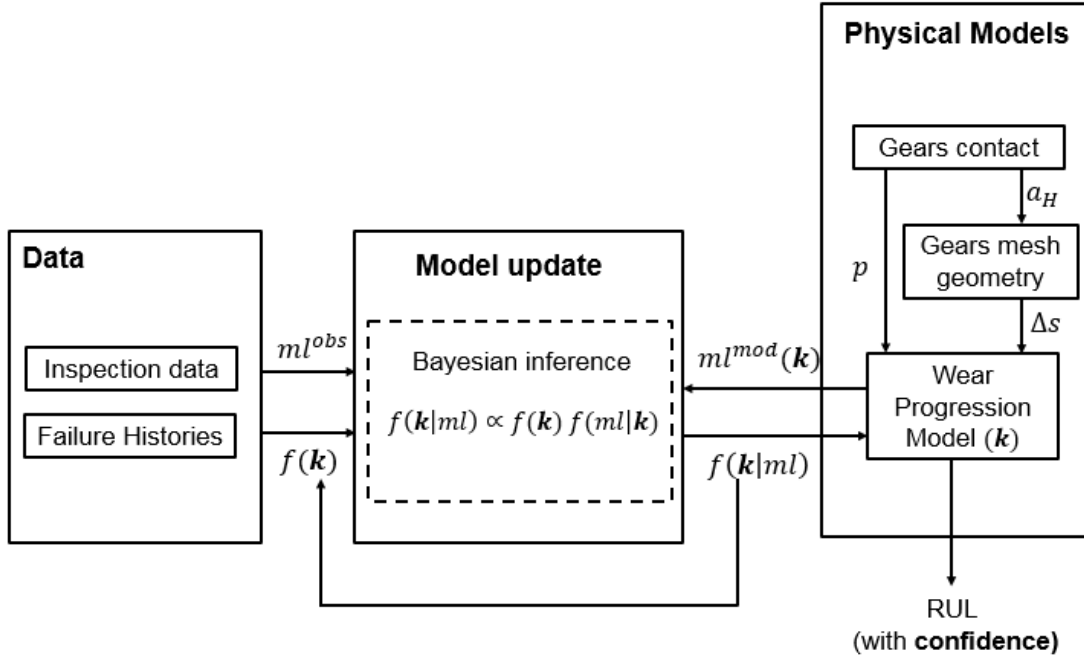


Figure 1. Framework of integrated prognostic method for gear wear prediction

### 3. Physical models in gear wear prediction

In this section, physical quantities that are needed to implement Archard' model and Bayesian inference are computed, which include contact pressure  $p$ , sliding distance  $s$  and the mass loss  $ml$ .

#### 3.1 Contact pressure and sliding distance

During the mesh process of gears, there is a relative movement between the two meshing teeth because of the difference in tangential velocity, except for the pitch point in spur gears. The sliding movement causes wear of gear surface. The material particles will be removed due to the surface wear and the tooth profile will be altered. As discussed before, the Archard wear model describes the wear rate. We can discretize the model into the form in (2)

$$h(i) = h(i - 1) + kp(\Delta s) \quad (2)$$

In order to use Archard's wear model to predict the gear surface wear, two important quantities are needed: the contact pressure and the sliding distance of all the points on the tooth flank during the mesh process. In order to analyze the two quantities for all the points on the tooth flank, a coordinate system is established first. In this coordinate system, the origin is located at the pitch point;  $y$  axis is along the line of action;  $x$  axis is perpendicular to the  $y$  axis. For spur gear with involute tooth profile, the contact points are moving along the  $y$  axis. As shown in Figure 2,  $P$  is the pitch point;  $B_1$  and  $B_2$  are the tangential touch points of base cycles; the tooth comes into mesh at point  $Q_2$  and departs the engagement at point  $Q_1$ ; the two points  $Q'_2$  and  $Q'_1$  are the transition positions for the two type of contacts: single-pair-contact and double-pair-contact. The load carried by this tooth is plotted above the  $y$  axis without scale.

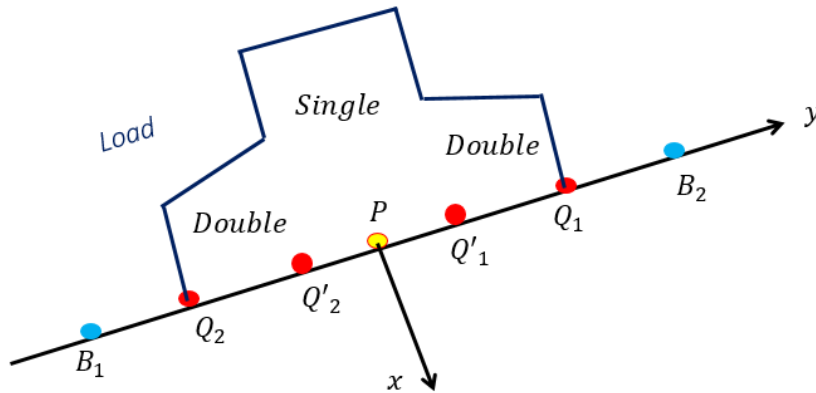


Figure 2. The coordinate system and the load distribution

When the meshing gears are loaded together by transmission load  $F$ , the surface will deform to form the area of contact, as shown in Figure 3. The contact can be regarded as the cylinder on cylinder line contact. Hertz contact theory will be applied to calculate the contact pressure for each point on tooth flank when it comes into mesh. Suppose one point on the tooth flank starts

the engagement at point  $N$  which has the coordinate of  $(0, y)$ . As shown in Figure 3, the contact width is  $2a_H$ . The radiuses of curvature at the contact point for the pinion and gear are  $R_1$  and  $R_2$  respectively.

$$R_1 = R_{b1} \tan \alpha_0 + y, \quad (3)$$

$$R_2 = R_{b1} \tan \alpha_0 - y, \quad (4)$$

The effective radius of curvature  $R^*$  is defined as

$$\frac{1}{R^*} = \frac{1}{R_1} + \frac{1}{R_2}. \quad (5)$$

In a similar manner, the effective modulus of elasticity  $E^*$  is defined as

$$\frac{1}{E^*} = \frac{1 - \nu_1^2}{E_1} + \frac{1 - \nu_2^2}{E_2}. \quad (6)$$

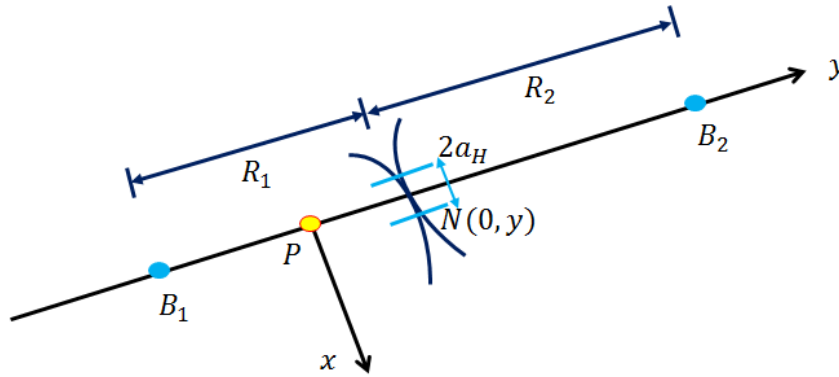


Figure 3. Contact of a pair of teeth

According to Hertz contact theory, the half contact width is

$$a_H = \sqrt{\frac{4FR^*}{\pi E^*}} \quad (7)$$

and the mean contact pressure is

$$\bar{P}_N = \frac{4F}{3\pi a_H} \quad (8)$$

After obtaining the contact pressure, another quantity that is needed in Archard's wear model is the sliding distance. Ref [21] gave an analytical formula for sliding distance  $s_1$  of the point  $N(0, y)$  on pinion flank as follows.

$$s_1 = a_H - \sqrt{(R_2)^2 - (R_{p2} \sin \alpha_0 - y_{1d})^2} + R_{p2} \cos \alpha_0 \quad (9)$$

$$R_2 = \sqrt{(R_{p2} \cos \alpha_0 - a_H)^2 + (R_{p2} \sin \alpha_0 - y_{1e})^2} \quad (10)$$

$$y_{1e} = \sqrt{R_1 - (R_{p1} \cos \alpha_0 + a_H)^2} - R_{p1} \sin \alpha_0 \quad (11)$$

$$y_{1d} = \sqrt{R_1 - (R_{p1} \cos \alpha_0 - a_H)^2} - R_{p1} \sin \alpha_0 \quad (12)$$

$$R_1 = \sqrt{(R_{p1} \cos \alpha_0)^2 + (R_{p2} \sin \alpha_0 - y)^2} \quad (13)$$

With the contact pressure and the sliding distance available, the determination of wear coefficient is required before using Archard's model to predict wear depth evolution.

### 3.2 Mass loss of wear

The gear type we consider in this paper is spur gear, which has a symmetric geometry. Therefore, the volume of metal loss is equal to the area removed according to the wear depth in 2D multiplied by the thickness of the tooth. As wear accumulates, tooth profile will change due to material loss. Figure 4 depicts the 2D shape of the spur gear tooth, in which we use a dashed

line to represent the tooth profile after some wear accumulation. The shaded area between the original tooth profile and the new one is the area of material loss. This area can be approximated in the following way. First divide the tooth height vertically at the points where the wear depth is computed. Then calculate the area of the each small element using the wear depth and sum them up. The mass loss will be calculated by multiplying this area by the thickness of the tooth, and then by the density of the material.

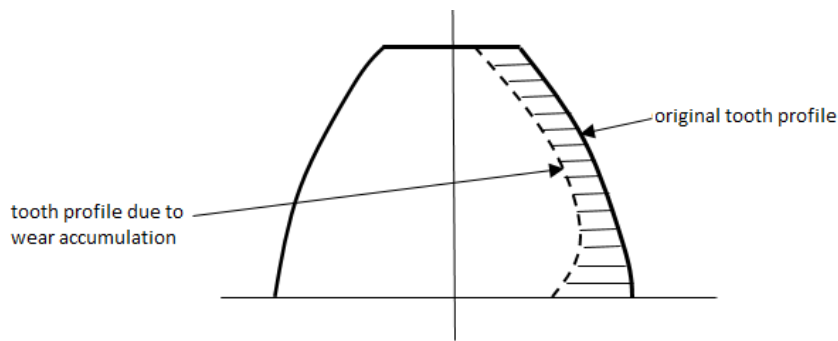


Figure 4. Area of material loss due to wear accumulation

#### 4. Model update through Bayesian inference

In this study, Archard's wear model is used to predict the wear depth evolution at each point on the tooth surface. More accurate wear coefficient in the model leads to more accurate wear prediction. However, different gears most likely have different wear evolution processes due to variations in material property, manufacturing process and working conditions. We therefore consider the wear coefficient as a random variable to account for the uncertainty in wear evolution process from the population point of view. Meanwhile, the health condition of a specific individual is of our interest. The uncertainty in failure time for an individual unit is much less than that for the population. Hence, a mechanism of uncertainty reduction is needed in

the wear prediction process. By noticing the material removal as a direct consequence of gear wear process, the gear mass loss would be a good indicator of wear status. The Bayesian inference will take the data on gear mass loss as observations to update the distribution of the wear coefficient. The formula for determining the posterior distribution of the uncertain parameter, wear coefficient  $k$ , is given as follows:

$$f_{post}(k|m) = \frac{l(m|k)f_{prior}(k)}{\int l(m|k)f_{prior}(k) dk} \quad (14)$$

where  $m$  represents the mass loss. The update on wear coefficient distribution is conducted at each inspection time when a new measurement of gear weight is available. The posterior distribution will serve as the prior distribution for the next update at the next inspection time.

At each inspection time  $T_j$ , the measured mass loss is  $m_j^{obs}$ . With the wear coefficient  $k^{j-1}$  obtained at the previous inspection time  $T_{j-1}$ , the predicted mass loss at inspection times  $T_1$  up to  $T_j$  are thus denoted by  $m_{1:j}^{mod}$ . We define the measurement error as  $e = m^{obs} - m^{mod}$  and assume it follows zero-mean Gaussian distribution with standard deviation  $\sigma$ . It is further assumed that the measurement errors at inspection times are identical and independently distributed. Thus, the likelihood to observe the mass loss at inspection times up to  $T_j$  is

$$l(m_{1:j}^{obs}|k^{j-1}) = \prod_{i=1}^j \frac{1}{\sqrt{2\pi}\sigma} \exp\left(-\frac{(m_i^{obs} - m_i^{mod})^2}{2\sigma^2}\right) \quad (15)$$

where  $m_{1:j}^{obs}$  represents the measured mass loss at inspections times  $T_1$  up to  $T_j$ .

In this paper, the prior in the Bayesian formula is assumed to be known and represents the knowledge of the wear process of the gear population. The prior can be obtained using the

following way in practice. For example, we suppose that  $N$  degradation paths from  $N$  test units are available. For each path, we use least square to obtain an estimate for the coefficient. Then we use Gaussian distribution to fit these  $N$  coefficients. Then this Gaussian distribution will be used as a prior distribution in the Bayesian equation. When no or little prior information on the failure history is known, it is more reasonable to use a non-informative prior.

## **5. Validation using planetary gearbox run-to-failure experiments**

Planetary gearbox is extensively used in helicopters, wind turbines and other systems which require high power transmission and good torque ratio in a small volume. The three types of gears involved are called sun gear, planet gear and ring gear. By changing the running state (stationary, rotation, or revolution) of each gear type, the planetary gearbox can have different configurations. The configuration to be investigated in this experiment is to keep ring gear stationary and provide power to the sun gear. All the gears are spur type.

Run-to-failure experiments in the lab environment were conducted using a planetary gearbox test rig, shown in Figure 5, hosted by the Reliability Research Lab at the University of Alberta. In this experiment, data collected include vibration signals, current signals of the drive/load motor, encoder signal and torque signal. In addition, the metal particle counter data and the weight loss of gears were also recorded. The physical parameters of this planetary gear set are listed in Table 1. More details on this experiment can be found in technical report [48]. Among all the gears, sun gear, as the driving gear, experiences the most severe wear. Therefore, the wear of the sun gear is of interest to study.



Figure 5. Planetary gearbox test rig [48]

Table 1. The physical parameters of the planetary gear set [48]

Parameters	Sun gear	Planet gear	Ring gear
Number of teeth	19	31	81
Module (mm)	3.2	3.2	3.2
Pressure angle	20°	20°	20°
Mass (kg)	0.7	1.822	5.982
Face width (m)	0.0381	0.0381	0.0381
Young's modulus (Pa)	$2.068 \times 10^{11}$	$2.068 \times 10^{11}$	$2.068 \times 10^{11}$
Poisson's ratio	0.3	0.3	0.3
Base circle radius (mm)	28.3	46.2	120.8

Before the gear was considered failed, the planetary gearbox experienced 19 runs. Each run had different durations. For example, run #1 lasted 8 hours 22 minutes, run #5 lasted 32 hours. The photographs in Figure 6 show the tooth profile changes of the sun gear during this experiment. In these photographs, we can see the gear tooth became thinner gradually as runs continued and more material were removed. At the end of run #19, the thickness of the teeth was

reduced to about 50% of the original thickness. According to the tooth profile changes and the metal particle data, this run-to-failure experiment can be divided into three stages:

- Runs 1-6: Normal operations to damage initiation
- Runs 7-11: Initial to severe damage progression
- Runs 12-19: Severe damage progression and profile change.

The weight loss of the sun gear is plotted in Figure 7. During these 19 runs, the input torque was kept to a constant level starting from run #5. Also considering the experiment set up process and the relatively large measurement error in the early stage, the data on the weight loss during run #1 to run #4 are not used in the validation.

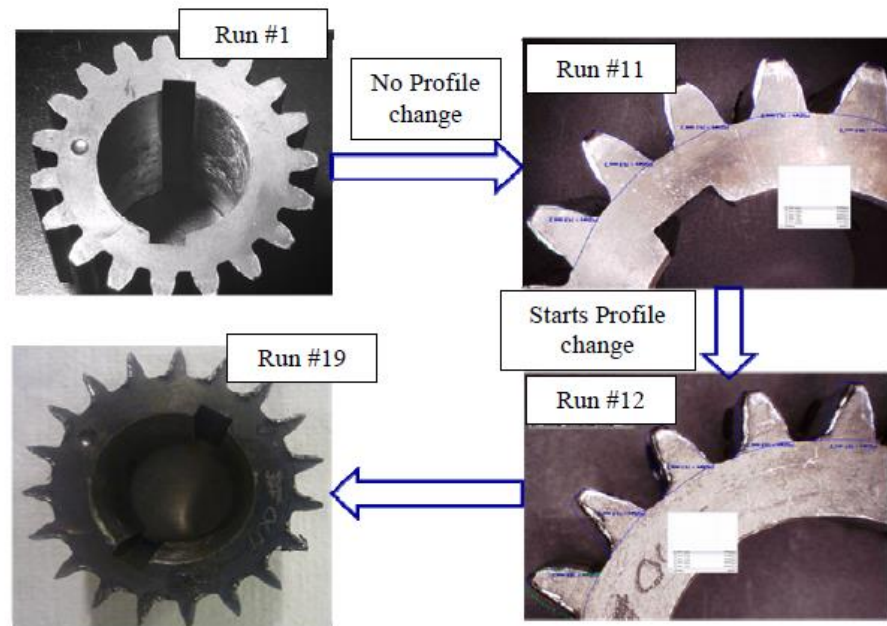


Figure 6. Tooth profile changes of the sun gear [48]

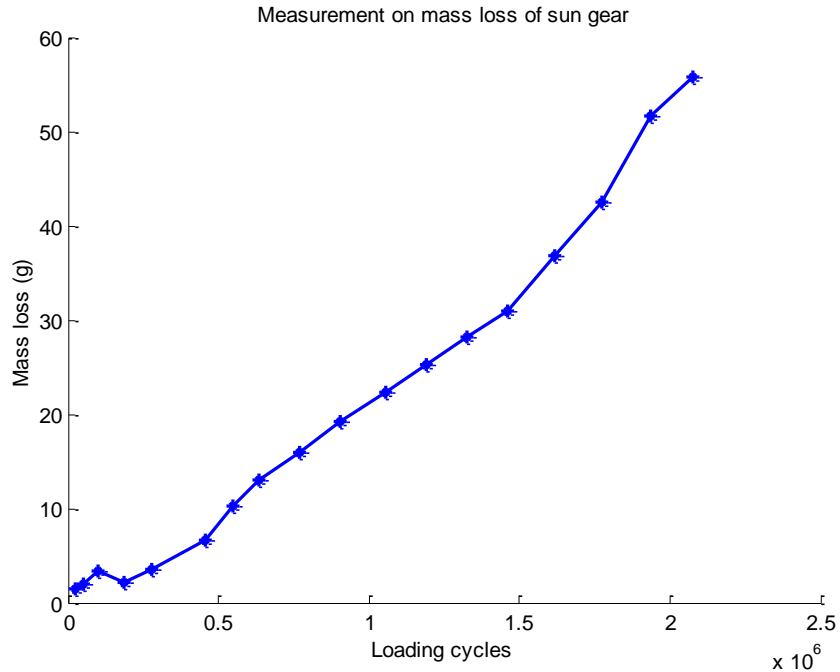


Figure 7. Measured mass loss of the sun gear

The contact pressure and sliding distance for each point on the sun gear tooth flank are calculated based on the methods given in Section 3. The contact pressure and the sliding distance for each point on tooth surface are assumed to be constant along the wear progression. During the late stages after run #14, we believe that this assumption is not valid anymore because the wear rate is accelerating and the predicted mass loss will be less than the actual mass loss. Therefore, for the purpose of validating the integrated prognostics method, the mass loss records from run #5 to run #14 are used to update the wear coefficient.

Starting from run #5, the input torque is fixed at 25 klb-in with the drive motor speed of 1200 rpm. When the sun gear and one planetary gear are meshing, there are two contact types: single-pair-contact and double-pair-contact. Under such condition, the static load on the sun gear is shown in Figure 8.

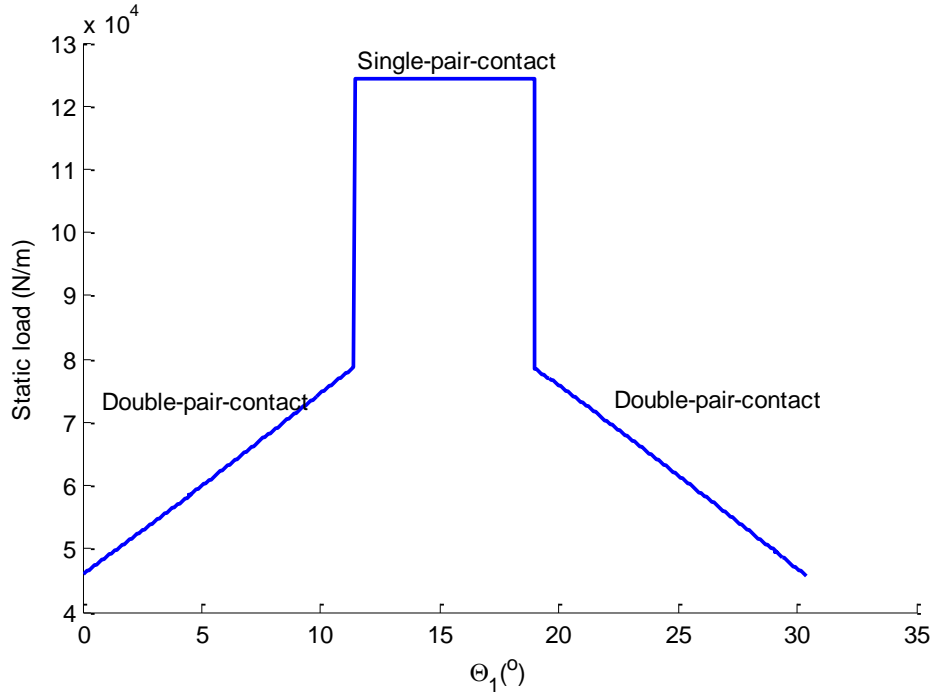


Figure 8. Static load on sun gear tooth

In addition, the gear mesh process is actually a combination of rolling and sliding contact. Beside surface wear due to sliding contact, the material removal is also contributed by rolling contact fatigue. During the experiment, pitting was observed on the gear tooth which was caused by rolling contact. To account for the effect of pitting on the mass loss, we select the maximum wear depth as the wear depth for all the points. The reason is that, in the photograph of tooth profile, the wear volume change is roughly uniform for all the points on the tooth flank. Furthermore, we assume that all the teeth of sun gear experience the same amount of wear because the photograph suggests similar wear condition in all the teeth of the sun gear. According to the configuration of the planetary gearbox, each tooth on the sun gear will mesh 3.2 times with all the four planet gears during one cycle of rotation. Hence, if we denote the wear depth in one mesh period of sun gear as  $h_s$  and the mass removed as  $m(h_s)$ , the total mass loss of the sun gear within one cycle of rotation will be  $m(h_s) \times 3.2 \times 19$  (# of teeth of sun gear).

For a given value of wear coefficient, we can use discretized Archard's model (2) to predict the wear depth. For example, when  $k = 1.27 \times 10^{-15} \text{Pa}^{-1}$ , Figure 9 displays the predicted wear depth from run #5 to run #14 by considering sliding wear effect only. From the figure, we can see that the maximum wear depth occurs near the tooth root area.

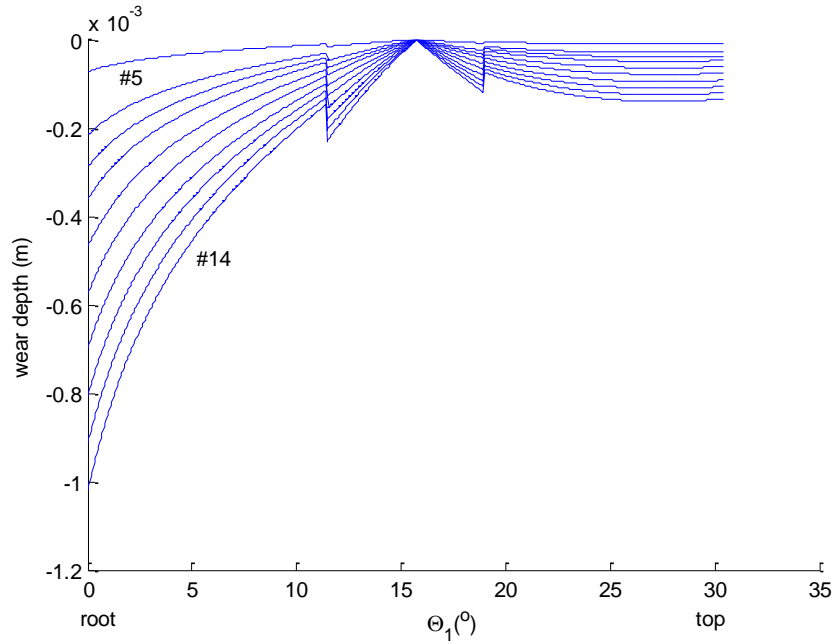


Figure 9. Predicted wear depth for the sun gear

Next, the update process for wear coefficient is presented. We consider two priors. One is Gaussian prior, and the other is uniform prior.

First, the prior distribution of wear coefficient  $k$  is assumed to follow Gaussian distribution  $N(3 \times 10^{-15}, (1 \times 10^{-15})^2)$ , and the measurement error follows another Gaussian distribution  $N(0, 0.5^2)$ . By selecting the maximum wear depth as the wear depth for all the points, the predicted mass loss is calculated at every inspection time. By applying Bayesian update formula

in (14) and (15), the update process is tabulated in Table 2. The updated distributions of the wear coefficient are shown in Figure 10.

Table 2. Update process for wear coefficient  $k$  (with Gaussian prior)

Run #	Cycles	Measured mass loss	Mean of $k$	Std of $k$
		0	3e-15	1e-15
5	89600	1.4	1.0552e-15	2.9315e-16
6	268800	4.45	0.9288e-15	9.2107e-17
7	358400	8.12	1.0664e-15	4.9948e-17
8	448000	10.9	1.1636e-15	3.2156e-17
9	582400	13.81	1.2186e-15	2.2289e-17
10	716800	17	1.2513e-15	1.6210e-17
11	868000	20.13	1.2672e-15	1.2228e-17
12	1002400	23.14	1.2748e-15	9.5061e-18
13	1136800	26.04	1.2776e-15	7.5751e-18
14	1271200	28.71	1.2770e-15	6.1681e-18

From the results of update process, it is observed that the mean of wear coefficient  $k$  has been adjusted from the prior value  $3 \times 10^{-15} \text{Pa}^{-1}$  to the value around  $1.27 \times 10^{-15} \text{Pa}^{-1}$ . Moreover, the shape of the distribution gets narrower, which indicates that the uncertainty is reduced gradually as more data of mass loss are available.

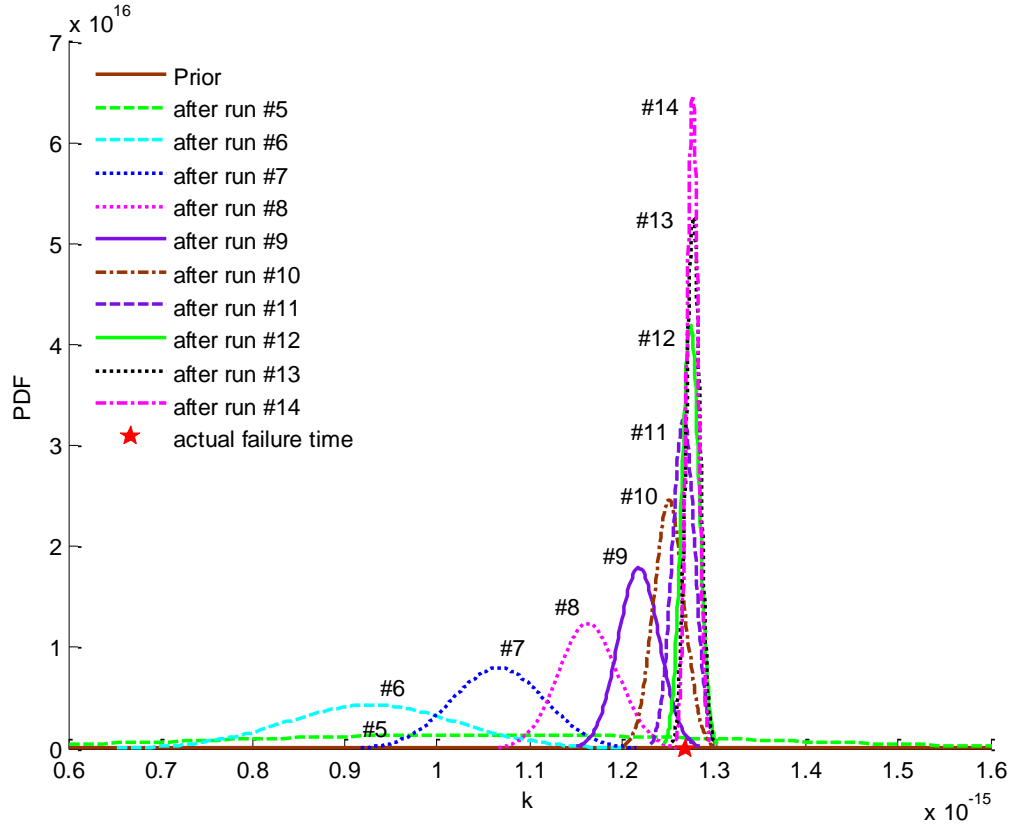


Figure 10. Updated distributions of wear coefficient  $k$

Next, we use uniform distribution as the prior distribution in the Bayesian updates. We select the uniform distribution ( $\sim \text{Uniform}(1.2679e-15, 4.7321e-15)$ ), which has the same mean and variance as the Gaussian distribution used in the original manuscript, as the prior in the Bayesian update. The updates of the wear coefficient is tabulated in the Table 3, from which we can see the mean of posterior distribution gradually converges to the value of around  $1.28e-15$  as more measurements arrive. Recall that the Bayesian updates using Gaussian prior eventually gave us the mean parameter value of  $1.27e-15$ . This fact tells that non-informative prior achieve similar parameter estimation as the Gaussian prior.

Table 3. Update process for wear coefficient  $k$  (with uniform prior)

Run #	Cycles	Measured mass loss	Mean of $k$	Std of $k$
		0	3e-15	1e-15
5	89600	1.4	1.4156e-15	1.2782e-16
6	268800	4.45	1.2947e-15	2.3659e-17
7	358400	8.12	1.2911e-15	2.0243e-17
8	448000	10.9	1.2962e-15	2.2081e-17
9	582400	13.81	1.2979e-15	2.0758e-17
10	716800	17	1.3010e-15	1.9463e-17
11	868000	20.13	1.2966e-15	1.5996e-17
12	1002400	23.14	1.2922e-15	1.3345e-17
13	1136800	26.04	1.2873e-15	1.1187e-17
14	1271200	28.71	1.2810e-15	8.5426e-18

As the wear coefficient gets more accurate, the failure time can be predicted with increased accuracy accordingly when a failure threshold is given. We consider the instance of Gaussian prior here and the similar result holds for uniform prior. In this example, we take the mass loss after run #14 (28.71g) as the failure threshold. With such threshold, the actual failure time will be at 1,271,200 cycles as recorded in the experiment, also indicated in Table 2. Figure 11 shows the update process for the failure time prediction using the updated wear coefficient in Figure 10. As expected, the distribution converges to the actual failure time with reduced uncertainty.

The prediction results are compared between the physics-based method and the integrated prognostics method, shown in Figure 12. The green dotted line with triangle marks represents the mass loss predicted by the physics-based method, which uses a prior value of wear coefficient  $k = 3 \times 10^{-15} \text{Pa}^{-1}$ . While, the red dashed line with circle marks represents the mass loss

predicted by the integrated prognostics method, which uses the mean value of posterior distribution of the wear coefficient in the last update  $k = 1.27 \times 10^{-15} \text{Pa}^{-1}$ . From the figure, it is obvious that the predicted results obtained by the integrated prognostics method agree well with the measured data from run #5 and run #14. In contrast, there is large discrepancy between the mass loss predicted by the physics-based method and the measured data. The results show that the integrated prognostics method is able to accurately estimate the wear coefficient for a specific unit under monitoring by using measurement on gear mass loss. With the updated wear coefficient obtained through Bayesian inference, the wear process and subsequently the failure time can be predicted in a more accurate fashion.

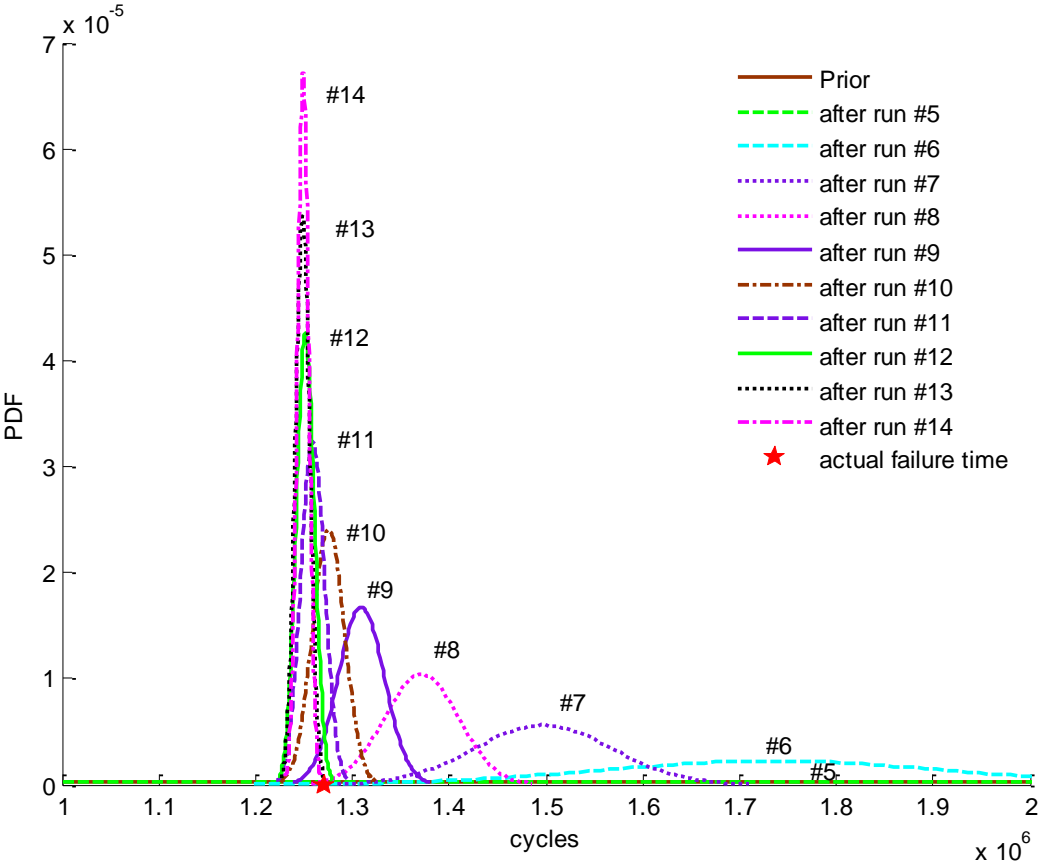


Figure 11. Updated distributions for failure time.

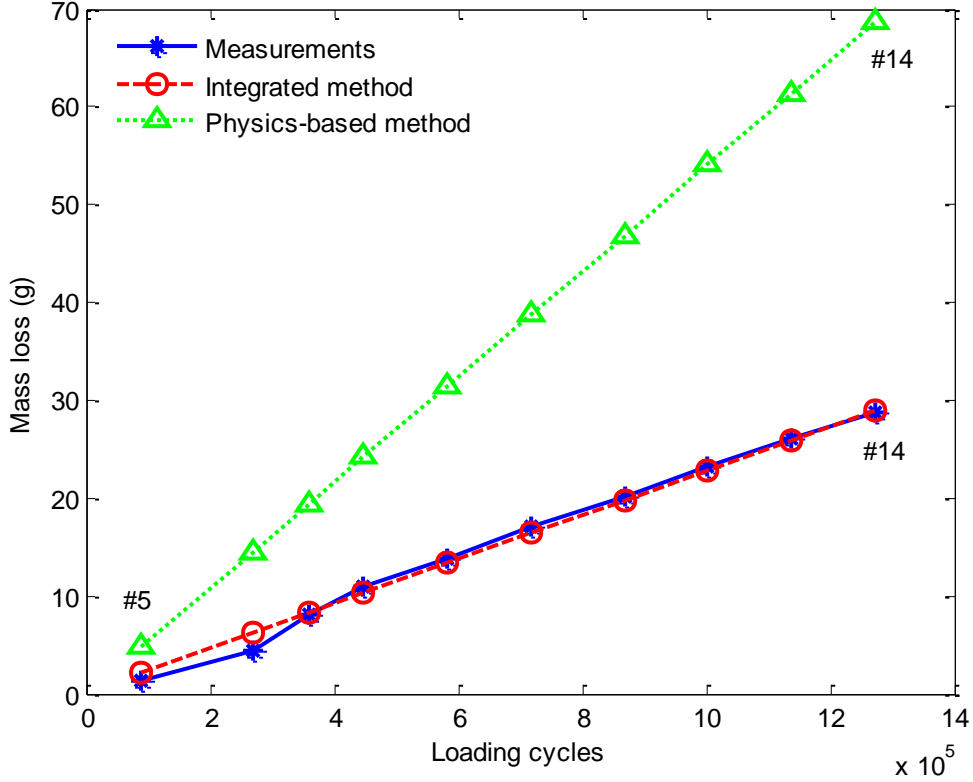


Figure 12. Comparison between the integrated method and physics-based method

The proposed integrated method is also compared with data-driven methods for predicting mass loss and RUL. Data-driven methods do not rely on physical models, and use condition monitoring data only to refine prediction models. We consider a popular type of data-driven prognostic model based on Bayesian inference and generic degradation models [11], [49], which have been applied in various applications. The degradation model adopted in reference [11] and [49] was exponential degradation model, with the following form:

$$L(t_i) = \alpha + \beta t_i + \varepsilon \quad (16)$$

where  $t_i$  is the inspection cycle,  $L(t_i)$  is the logarithm of the measurement data, i.e., metal loss in this case study.  $\alpha$  and  $\beta$  are uncertain parameters to be updated, and  $\varepsilon$  is the error term. Suppose the prior distributions of the uncertain parameters can be estimated based on historical data or

knowledge, and the prior distribution of  $\alpha$  is specified to be  $N(0, 0.3^2)$ , and the prior distribution of  $\beta$  is set to be  $N(1 \times 10^{-5}, 0.3 \times 10^{-5^2})$ .  $\varepsilon$  follows normal distribution  $N(0, 0.1^2)$ . Based on the collected metal loss data, Bayesian inference is applied to update the uncertain parameters  $\alpha$  and  $\beta$ , and thus metal loss prediction can be refined.

We also considered another degradation function, linear degradation function, because of the shape of the metal loss degradation path, which takes the following form:

$$ML(t_i) = a + bt_i + \varepsilon \quad (17)$$

where  $ML(t_i)$  is the metal loss measurement data,  $a$  and  $b$  are uncertain parameters to be updated, and  $\varepsilon$  is the error term. Suppose the prior distribution of  $a$  is specified to be  $N(0, 0.3^2)$ , and the prior distribution of  $\beta$  is set to be  $N(1 \times 10^{-5}, 0.3 \times 10^{-5^2})$ .  $\varepsilon$  follows normal distribution  $N(0, 0.1^2)$ . Bayesian inference is applied to update the uncertain parameters  $a$  and  $b$  based on the metal loss data, to refine metal loss predictions.

The metal loss prediction results using integrated method and the above two data-driven methods are presented in Figure 13, from which we can see clearly that using the coefficient obtained by the last update, integrated method gives more accurate mass loss prediction. In Figure 14, we plot the RUL error (defined as the difference between the predicted RUL and the real RUL) at every inspection time. The comparison shows that the integrated method using uniform prior in the Bayesian update performs best for this specific degradation in that it gives smallest RUL prediction error starting from very early stage. The comparative study results show that the proposed integrated method can results in more accurate wear propagation prediction comparing to the popular data-driven methods based on Bayesian inference and generic degradation models.

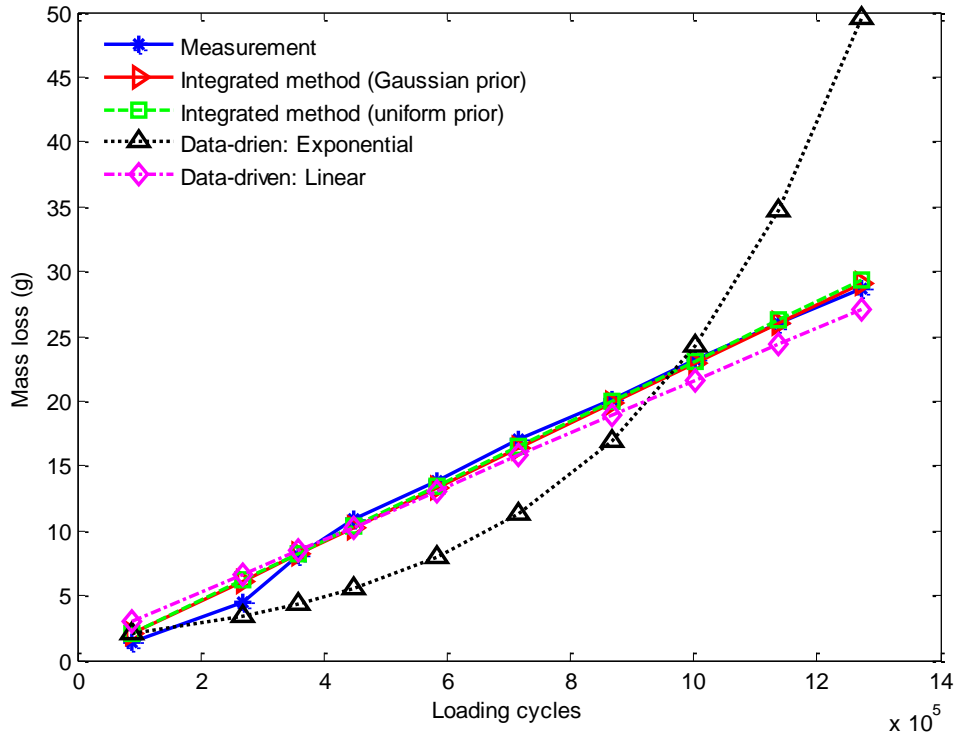


Figure 13. Comparison of mass loss prediction between the integrated method and data-driven methods

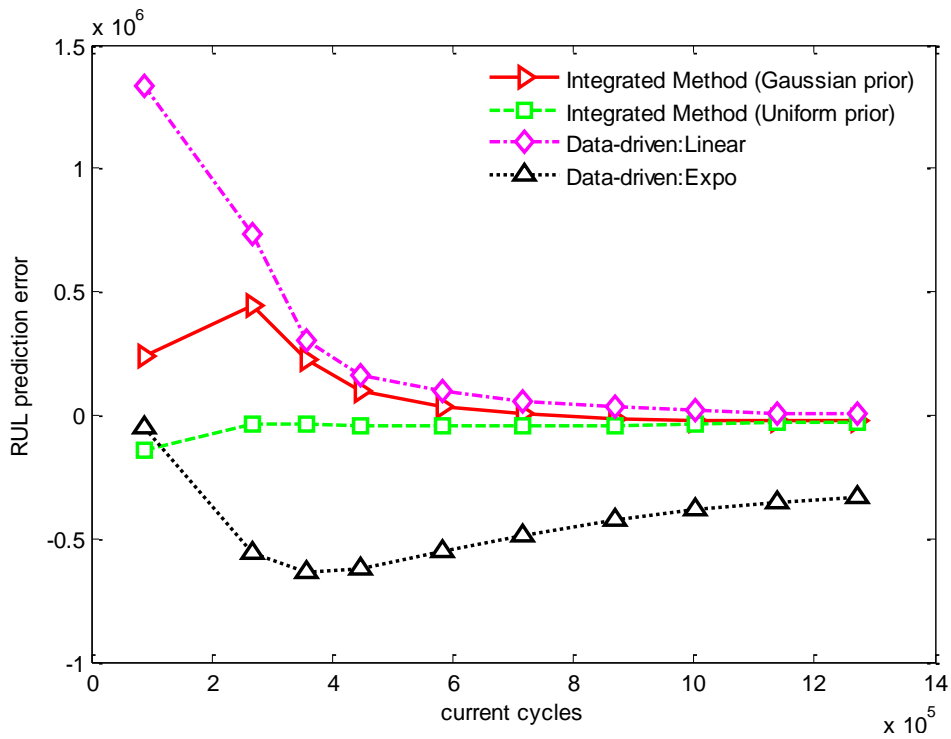


Figure 14. Comparison of RUL prediction error between the integrated method and data-driven methods

## **6. Conclusions and future work**

In this paper, an integrated prognostics method is proposed for failure time prediction of gears subject to surface wear failure mode, utilizing both physical models and condition monitoring data. Comparing to existing physics-based gear wear prediction methods which use fixed wear coefficient, the proposed integrated method can result in more accurate estimate of wear coefficient distribution for the individual gear unit being monitored, and thus lead to more accurate failure time prediction. The proposed method is validated using gearbox run-to-failure experiments, and compared with the physics-based methods and data-driven methods.

The wear model is used to predict the surface wear due to sliding contact. In order to account for the contribution of rolling contact to the mass loss, we propose to remove the material using the maximum wear depth. In the future, we may investigate the physical mechanism to account for the interactions between pitting and surface wear processes. In addition, the assumption of constant contact pressure and sliding distance does not seem to be suitable anymore for the late stage of the wear process with severe profile change. We plan to further investigate how to account for the effects of tooth profile changes due to material removal, and develop gear dynamic model with high fidelity to simulate the gear mesh process, as well as method to calculate the increased varying contact pressure, with the presence of significant gear profile change. Such degradation pattern change results in a change-point in the degradation path. If we have failure histories of multiple units, all with similar degradation pattern with such change-point, two-phase change-point regression models will be effective candidates for locating the

change-point position [50-52], which will support identifying which physical models to utilize in the integrated prognostics approach and predicting the gear remaining life.

## Acknowledgment

This research was partially supported by the Natural Sciences and Engineering Research Council of Canada (NSERC). We greatly appreciate the help from Dr. Ming Zuo and the Reliability Research Lab at the University of Alberta for providing the gearbox experiment data used in the case study.

## References

- [1] P. Bajpai, A. Kahraman, and N. E. Anderson, "A surface wear prediction methodology for parallel-axis gear pairs," *J. Tribol.*, vol. 126, no. 3, pp. 597–605, 2004.
- [2] P. C. Paris, F. Erdogan, "A critical analysis of crack propagation laws," *Journal of Basic Engineering* vol. 85, pp. 528-534, 1963.
- [3] D. G. Lewicki, R. Ballarini, "Gear crack propagation investigations," *Tribotest journal*, vol. 5, pp. 157-172, 1998.
- [4] D. G. Lewicki, R. F. Handschuh, L. E. Spievak, P. A. Wawrzynek, A. R. Ingraffea, "Consideration of moving tooth load in gear crack propagation predictions," *Transactions of the ASME*, vol. 123, pp. 118-124, 2001.
- [5] H. Liebowitz, E. T. Moyer, "Finite element methods in fracture mechanics," *Computers & Structures*, vol. 31, pp. 1-9, 1989.
- [6] R. D. Henshell, K. G. Shaw, "Crack tip finite elements are unnecessary," *International journal for numerical methods in engineering*, vol. 9, pp. 495-507, 1975.
- [7] R. S. Barsoum, "On the use of isoparametric finite elements in linear fracture mechanics," *International journal for numerical methods in engineering*, vol. 10, pp. 25-37, 1976.
- [8] C. J. Li, H. Lee, "Gear fatigue crack prognosis using embedded model, gear dynamic model and fracture mechanics," *Mechan Syst Signal Process*, vol. 19, pp. 836-846, 2005.
- [9] G.J. Kacprzynski, A. Sarlashkar, M. J. Roemer, A. Hess, G. Hardman, "Predicting remaining life by fusing the physics of failure modeling with diagnostics," *J Minerals Metals Mater Soc*, vol. 56, pp. 29-35, 2004.
- [10] D. Banjevic, A. K. S. Jardine, V. Makis, M. Ennis, "A control-limit policy and software for condition-based maintenance optimization," *INFOR*, vol. 39, pp. 32-50, 2001.

- [11] N. Gebraeel, M. A. Lawley, R. Li, J. K. Ryan, "Life distributions from component degradation signals: a Bayesian approach," *IIE Trans Qual Reliab Eng*, vol. 37, pp. 543-557, 2005.
- [12] N. Gebraeel, M. A. Lawley, "A neural network degradation model for computing and updating residual life distributions," *IEEE Trans Autom Sci Eng*, vol. 5, pp. 154-163, 2008.
- [13] Z. Tian, L. Wong, N. Safaei, "A neural network approach for remaining useful life prediction utilizing both failure and suspension histories," *Mechan Syst Signal Process*, vol. 24, pp. 1542-1555, 2010.
- [14] W. Q. Wang, M. F. Golnaraghi, F. Ismail, "Prognosis of machine health condition using neuro-fuzzy systems," *Mechanical Systems and Signal Processing*, vol. 18, pp. 813-831, 2004.
- [15] Z. Tian, M. J. Zuo, "Health condition prediction of gears using a recurrent neural network approach," *IEEE Transactions on Reliability*, vol. 59, pp. 700-705, 2010.
- [16] Z. Xi, R. Jing, P. Wang, C. Hu, "A copula-based sampling method for data-driven prognostics," *Reliability Engineering and System Safety*, vol. 132, pp. 72-82, 2014.
- [17] A. Coppe, R. T. Haftka, N. H. Kim, "Uncertainty reduction of damage growth properties using structural health monitoring," *J Aircraft*, vol.47, pp. 2030-2038, 2010.
- [18] D. An, J. Choi, N. H. Kim, "Identification of correlated damage parameters under noise and bias using Bayesian inference," *Struct Health Monit*, vol. 11, pp. 293-303, 2012.
- [19] F. Zhao, Z. Tian, Y. Zeng, "Uncertainty quantification in gear remaining useful life prediction through an integrated prognostics method," *IEEE Trans Reliab*, vol. 62, pp. 146-159, 2013.
- [20] F. Zhao, Z. Tian, Y. Zeng, "A stochastic collocation approach for efficient integrated gear health prognosis," *Mechan Syst Signal Process*, vol. 39, pp. 372-387, 2013.
- [21] F. Zhao, Z. Tian, E. Bechhoefer, Y. Zeng, "An integrated prognostics method under time-varying operating conditions," *IEEE Trans Reliab*, vol. 64, pp.673-686, 2015.
- [22] S. Marble, B. P. Morton, "Predicting the remaining life of propulsion system bearings," in *Proc 2006 IEEE Aerospace Conf, Big Sky, MT, USA, 2006*.
- [23] E. Bechhoefer, "A method for generalized prognostics of a component using Paris law," *Annual forum proceedings-American helicopter society 2008*; 64 (2), 1460
- [24] M. E. Orchard, G. J. Vachtsevanos, "A particle filtering approach for on-line failure prognosis in a planetary carrier plate," *Int J Fuzzy Logic Intell Syst*, vol. 7, pp. 221-227, 2007.
- [25] M. E. Orchard, G. J. Vachtsevanos, "A particle filtering-based framework for real-time fault diagnosis and failure prognosis in a turbine engine," presented at the 2007 Mediterranean Conf on Contr Autom, Athens, Greece, 2007.
- [26] E. Zio, G. Pelsoni, "Particle filtering prognostic estimation of the remaining useful life of nonlinear components," *Reliab Eng Syst Safe*, vol. 96, pp. 403-409, 2011.
- [27] J. Archard, "Contact and rubbing of flat surfaces," *J. Appl. Phys.*, vol. 24, no. 8, pp. 981-988, 1953.
- [28] S. M. Hsu, M. C. Shen, and A. W. Ruff, "Wear prediction for metals," *Tribol. Int.*, vol. 30, no. 5, pp. 377-383, 1997.
- [29] J. A. Williams, "Wear modelling: analytical, computational and mapping: a continuum mechanics approach," *Wear*, vol. 225, pp. 1-17, 1999.
- [30] Y.-W. Zhao, J.-J. Liu, and L.-Q. Zheng, "The friction and wear model of steels and their probable statistic calculations," *Tribol. Trans.*, vol. 35, no. 4, pp. 673-678, 1992.
- [31] K. Kato, "Abrasive wear of metals," *Tribol. Int.*, vol. 30, no. 5, pp. 333-338, 1997.
- [32] S. Wu and H. S. Cheng, "A sliding wear model for partial-EHL contacts," *J. Tribol.*, vol. 113, no. 1, pp. 134-141, 1991.
- [33] W. Yan, N. P. O'Dowd, and others, "A micromechanics investigation of sliding wear in coated components," in *Proceedings of the Royal Society of London A: Mathematical, Physical and Engineering Sciences*, 2000, vol. 456, pp. 2387-2407.

- [34]M. A. Ashraf, B. Sobhi-Najafabadi, M. G. Ellis, and H. Y. Hsu, Modeling of dry sliding wear using a systematic approach, vol. 324. Trans Tech Publ, 2006.
- [35]J. Abdo, “Materials Sliding Wear Model Based on Energy Dissipation,” *Mech. Adv. Mater. Struct.*, vol. 22, no. 4, pp. 298–304, 2015.
- [36]J. F. Molinari, M. Ortiz, R. Radovitzky, and E. A. Repetto, “Finite-element modeling of dry sliding wear in metals,” *Eng. Comput.*, vol. 18, no. 3/4, pp. 592–610, 2001.
- [37]M. A. Ashraf, R. Ahmed, O. Ali, N. H. Faisal, A. M. El-Sherik, and M. F. A. Goosen, “Finite Element Modeling of Sliding Wear in a Composite Alloy Using a Free-Mesh,” *J. Tribol.*, vol. 137, no. 3, p. 31605, 2015.
- [38]R. G. Buentello-Hernandez and A. Palazotto, “Development of a Model Considering High-Speed Sliding Wear,” *J. Aerosp. Eng.*, vol. 28, no. 5, p. 4014140, 2014.
- [39]J. F. Lin and C. C. Chou, “The response surface method and the analysis of mild oxidational wear,” *Tribol. Int.*, vol. 35, no. 11, pp. 771–785, 2002.
- [40]M. C. M. Farias, R. M. Souza, A. Sinatora, and D. K. Tanaka, “The influence of applied load, sliding velocity and martensitic transformation on the unlubricated sliding wear of austenitic stainless steels,” *Wear*, vol. 263, no. 1, pp. 773–781, 2007.
- [41]H. K. Durmuş, E. Özkaya, C. Meri, and others, “The use of neural networks for the prediction of wear loss and surface roughness of AA 6351 aluminium alloy,” *Mater. Des.*, vol. 27, no. 2, pp. 156–159, 2006.
- [42]Z. Zhang, N.-M. Barkoula, J. Karger-Kocsis, and K. Friedrich, “Artificial neural network predictions on erosive wear of polymers,” *Wear*, vol. 255, no. 1, pp. 708–713, 2003.
- [43]W. O. Winer and M. B. Peterson, *Wear Control Handbook*. American society of mechanical engineers, 1980.
- [44]S. Andersson, “Wear Simulation,” 2010.
- [45]A. Flodin and S. Andersson, “Simulation of mild wear in spur gears,” *Wear*, vol. 207, no. 1, pp. 16–23, 1997.
- [46]A. Flodin and S. Andersson, “Simulation of mild wear in helical gears,” *Wear*, vol. 241, no. 2, pp. 123–128, 2000.
- [47]S. Sankararaman, Y. Ling, and S. Mahadevan, “Uncertainty quantification and model validation of fatigue crack growth prediction,” *Eng. Fract. Mech.*, vol. 78, no. 7, pp. 1487–1504, 2011.
- [48]M. R. H. Van Tuan Do, A. Sahoo, M. Pandey, and M. J. Zuo, “Metal Scan Data, Gear Weight Loss Data, and Gear Damage Images Recorded during the Run-to-Failure Experiments,” Technical Report, University of Alberta, Edmonton, Alberta, Canada, 2010.
- [49] H. Liao and Z. Tian, “A framework for predicting the remaining useful life of a single unit under time-varying operating conditions,” *IIE Trans.*, vol. 45, no. 9, SI, pp. 964–980, Sep. 2013.
- [50] S. J. Bae, P. H. Kvam, “A change-point analysis for modeling incomplete burn-in for light displays,” *IIE. Trans.*, vol. 38, no. 6, pp. 489-498, 2006.
- [51] T.S. Ng, “An application of the EM algorithm to degradation modeling,” *IEEE Trans. Reliab.*, vol. 57, no. 1, pp. 2-13, 2008.
- [52] S. J. Bae, T. Yuan, S. Ning, W. Kuo, “ A bayesian approach to modeling two-phase degradation using change-point regression,” *Reliab. Eng. Syst. Saf.*, vol. 134, pp. 66-74, 2015.